Organic & Biomolecular Chemistry

Cite this: *Org. Biomol. Chem.*, 2012, **10**, 1834

www.rsc.org/obc

PAPER

Non-symmetrically substituted phenoxazinones from laccase-mediated oxidative cross-coupling of aminophenols: an experimental and theoretical insight†

Frédéric Bruyneel,[a] Georges Dive[b] and Jacqueline Marchand-Brynaert*[a]

Received 20th May 2011, Accepted 3rd November 2011
DOI: 10.1039/c1ob05795b

Oxidative cross-coupling reactions of substituted *o*-aminophenols were catalyzed by a commercial laccase to produce non-symmetrically substituted phenoxazinones for the first time. Identification by ^{1}H-, ^{13}C- and ^{31}P-NMR, and by HPLC-PDA and HPLC-MS/MS of exclusively two kinds of substituted phenoxazinones out of four potential heterocyclic frameworks was confirmed by a DFT study. The redox-properties of the substrates, their relative rates of conversion and the rigid docking of selected substrates led to a revisited mechanistic pathway for phenoxazinones biosynthesis. Our suggestions concern both the first formal two-electron oxidation by laccase and the first intermolecular 1,4-conjugated addition which secures the observed regioselectivity.

Introduction

The phenoxazinone framework containing a tricyclic iminoquinone core structure is widely distributed in natural products displaying remarkable biological activities and redox properties.[1–3] Along with some of the most potent antineoplastic agents (actinomycins), new antibiotics featuring a phenoxazinone structure are still regularly isolated from numerous fungal, bacterial or invertebrate sources (Fig. 1).[4–7] Notwithstanding the wide pool of natural organisms producing these heterocycles, a common biosynthetic pathway has emerged which involves enzymes from the class of multicopper oxidases (MCO).[2a,5–10] Among them, an increasing focus has been directed towards laccases [EC 1.10.3.2] because they are valuable biocatalysts in organic synthesis and green chemical processes.[11] Recent examples involve the laccase-mediated synthesis of cinnabarinic acid analogues, featuring phosphonylated or sulfonylated groups, as novel dyes and fluorophores.[9a,12] Some compounds endowed with tunable water-solubility were successfully used in a live-cell imaging application.[12d] Other heterocyclic frameworks displaying biological activities such as annulated benzofurans, phenazines and cycloheptenes were also recently synthesized.[13] The main advantage of those examples is the production by the laccase of an oxidized electrophile on which any less oxidizable nucleophile can

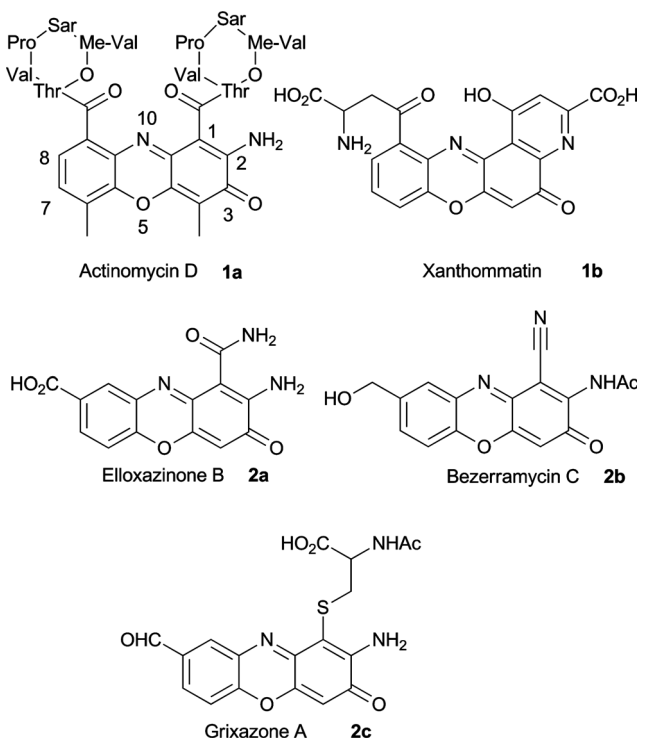

Fig. 1 Structures of natural products featuring the 2-aminophenoxazinone framework.

[a]*Institute of Condensed Matter and Nanosciences (IMCN), Organic and Medicinal Chemistry (CHOM), Université catholique de Louvain, Bâtiment Lavoisier, Place Louis Pasteur L4.01.02, 1348, Louvain-la-Neuve, Belgium. E-mail: jacqueline.marchand@uclouvain.be; Fax: +32(10)474168*
[b]*Centre d'ingénierie des Protéines, Université de Liège, Bâtiment B6, Allée du 6 Août, 4000, Sart-Tilman (Liège), Belgium*

† Electronic supplementary information (ESI) available: voltammograms, NMR spectra of isolated compounds, HPLC-PDA, MS, MS^2 spectra and identification description, docking results. See DOI: 10.1039/c1ob05795b

further react. Therefore the chemoselectivity of such catalytic processes is secured in the first step and this ensures a good yield of the final product. In the case of phenoxazinone derivatives, the oxidized electrophile is generated by the laccase from the nucleophilic partner itself which may reduce the molecular diversity.

In nature, the structural variability within the phenoxazinone series comes from the use of *o*-aminophenol precursors mainly differing in their oxidation states. This is often followed by site-selective acetylation and methylation reactions.[5a,7] Further structural modifications may arise from rare *N*-acetylcysteine nucleophilic substitution, aminolytic oxirane ring opening or transamination and dehydration steps.[7b]

Regarding the actinomycin-like phenoxazinones or the related xanthommatin framework (Fig. 1), the plausible synthetic pathway involves two identical precursors *i.e.* *o*-substituted aminophenols.[2a,14] Their natural transformations are realized either by a laccase, a phenoxazinone synthase or a tyrosinase.[10] The biosynthesis of grixazone, elloxazinones or bezerramycins A–C is thought to be slightly different.[5,7] In case of grixazone, part of the *o*-aminophenol is submitted to oxidation and nucleophilic substitution before reacting with the residual native *o*-aminophenol. Both elloxazinone B and bezerramycin C (Fig. 1) lack a substituent at C-9 but are functionalized at the C-8 and C-1 positions. This necessarily implies a selective coupling of two different precursors. Such transformation has not been realized to date in a laboratory with a laccase.[7]

As members of the blue multicopper oxidases, laccases and phenoxazinone synthases have been widely investigated to delineate the structural features of their catalytic sites.[15–17] It appears now that the phenoxazinone synthase isolated from *Streptomyces antibiocus* possesses a substrate binding pocket and solvent channels more similar to those of laccases than any other MCO.[18] These structural characteristics concern more precisely the four copper atoms distributed into the three sites named T1, T2 and T3.[15] The blue Cu-site (T1) holds an intense absorption around 600 nm due to the highly π covalent link between S (Cys) and Cu^{2+}. The copper is bound to two other ligands (His) to form the trigonal plane, whereas a fourth ligand, involved in the tuning of the enzyme activity, varies greatly among proteins. The T1 site is the primary acceptor of electrons; it is slightly buried in the enzyme core near the substrate binding cavity where small molecules are oxidized.[15,19] T2 and T3 copper sites form a trinuclear cluster where channelled electrons from T1 are transferred to molecular oxygen which is reduced to water. Recent X-ray crystallographic data of complexes containing both the enzyme and an aromatic substrate have shed some light upon the binding mode of small molecules into the cavity near the T1 site.[20] Contrary to tyrosinase, the substrate in laccase does not directly bind to the copper atom. The small molecule is involved in hydrogen bonds with one of the His ligands (His458) of the copper atom of the T1 site and probably to a Asp residue (Asp206) in the vicinity.[19] The rest of the cavity mostly contains hydrophobic residues which may also be involved in π–π stacking interactions.

The laccase-mediated synthesis of elaborated phenoxazinones endowed with fluorescent properties has only been recently investigated. The challenging problem of an oxidative cascade leading to selected non-symmetrically substituted fluorophores remains to be addressed. The present study focuses on the chemoselectivity of laccase-mediated coupling reactions of mixtures of *o*-aminophenol substrates, considering their steric, redox and electrophilic properties. The production of non-symmetrically substituted phenoxazinone dyes, in a controlled manner, could improve our understanding of the biosynthetic pathway mechanism. The use of cyclic voltammetry allowed to determine the ease of oxidation of the substrates. High-performance liquid chromatography systems equipped with either photodiode array detection (HPLC-PDA) or coupled to mass spectrometry (HPLC-MS) were used to identify the novel dyes.[21] The HPLC-PDA method helped to delineate the selectivity and to establish a relative scale for the conversion rates of selected substrates by laccase. Using the Density Functional Theory (DFT) method, we calculated how the regioselectivity may be secured in the first 1,4-addition step on the iminoquinone intermediate. The rigid docking of few substrates suggested a plausible explanation for one precursor failing to give the symmetrically substituted phenoxazinone.

Results and discussion

Oxidation potentials of the substrates

The set of substrates (*i.e.* substituted *o*-aminophenols **3–4**) chosen for this study was previously described regarding their chemical synthesis and "dimerization" into the corresponding symmetrically substituted phenoxazinones **5–6** (Table 1, Scheme 1).[12a,b,d] A relative reactivity scale was previously given based on isolated yields of oxidative dimerization products obtained with a commercial semi-purified laccase (referred to as **Tv1**) (Table 1, column 6). Moreover several kinetic data were collected with a similar laccase isolated and totally purified (Table 1, column 8). The intrinsic redox properties of compounds **3–4** were assessed now (Table 1, column 4) along with the conversion rates obtained using a surrogate commercial laccase preparation of lower cost (referred to as **Tv2**) (Table 1, column 7). Cyclic voltammetry was used to measure the relative ease of oxidation of the substrates.[21,22] The laccase natural substrate *i.e.*, 3-hydroxyanthranilic acid (**3a**, entry 1), well studied by electrochemical methods,[21,23] was included in the set as a reference. The interpretation of the cyclic voltammograms (given in ESI†) was based on previous studies dedicated to the redox-properties of kynurenine species (oxidized metabolites of tryptophan degradation) in aqueous buffer (pH 7).[23]

Like kynurenines (*e.g.* (*S*)-2-amino-4-(2-amino-3-hydroxyphenyl)- 4-oxo-butanoic acid), the aminophenols exhibited a distinct redox-behavior. A positive shift towards higher potential was observed here, due to the organic solvent used.[24] All substrates possess a marked oxidation peak and a very weak reduction one. A single wave corresponding to a two-electron transfer is observed along with the absence of a fully reversible redox behavior. The oxidation normally leads to a quinone-imine species and the absence of significant reduction peak indicates that this intermediate is highly reactive.[23] The results of Table 1 can be summarized as follows: all compounds exhibit similar oxidation potentials which are close to the one of the reference (entry 1, **3a**) and mostly fall within the experimental error. Sadly, neither the oxidation potential measured or the conversion yields

Table 1 The relative ease of oxidation of aminophenol precursors and their laccase-mediated conversions into phenoxazinones

Aminophenol precursors						Laccase-mediated synthesized heterocycles		
Entry	Fg		Cmpd	E_{pa}/V^a	Products[b] cmpd	Conv% (Yield%)-**Tv1**[c 12a,b,d]	Conv%-**Tv2**[d]	$K_m^{app\ e\ 12b}$
1	CO_2H	C_3	**3a**	1.03	**5a**	>70	>70	Nd
2	PO_3H_2	C_3	**3b**	0.98	**5b**	>95-(90)	>90	Nd
3	SO_3H	C_3	**3c**	1.00	**5c**	>95-(90)	>90	0.075 ± 0.008
4	SO_2NH_2	C_3	**3d**	1.03	**5d**	>80-(70)	>80	0.066 ± 0.001
5	SO_2NHPh	C_3	**3e**	1.03	**5e**	>70-(40)	Nd	Nd
6	$SO_2NHC_6H_{11}$	C_3	**3f**	1.04	**5f**	>90-(86)	>80	Na[f]
7	$SO_2NHCH_2CO_2Me$	C_3	**3g**	1.05	**5g**	>70-(58)	Nd	Nd
8	$SO_2NH(CH_2)_3$–OH	C_3	**3h**	0.98	**5h**	>90-(90)	Nd	Nd
9	$SO_2NH(CH_2)_2$–NH_2	C_3	**3i**	1.10	**5i**	>90-(87)	Nd	Nd
10	$SO_2NH(CH_2)_3$–NMe_2	C_3	**3j**	1.03	**5j**	>90-(90)	>80	0.069 ± 0.014
11	SO_3H	C_6	**4c**	0.96	**6c**	<20-(4)	<50	1.899 ± 0.313
12	$SO_2NHC_6H_{11}$	C_6	**4f**	1.02	**6f**	>80-(73)	>60	0.042± 0.003
13	$SO_2NH(CH_2)_3$–NMe_2	C_6	**4j**	0.98	**6j**	~0-(0)	~0	Nd

[a] Anodic peak of oxidation recorded by cyclic voltammetry in DMF with $TBABF_4$ as supporting electrolyte (± 0.02 V); [b] See Scheme 1 for general structure of the heterocyclic core; [c] **Tv1** = commercial *Trametes versicolor* laccase (Bioscreen® laccase). Conversions were estimated by HPLC-PDA and isolated yields of phenoxazinones were previously reported in literature.[12a,b,d]; [d] **Tv2** = commercial surrogate laccase from *Trametes versicolor* (Aldrich). Conversions were estimated by HPLC-PDA; Nd = not determined; [e] Kinetic data collected with purified laccase from *Pleurotus sajor caju* (28 U mL^{-1}) at pH 6–6.5;[12b f] Na = not available as the precursor is not fully soluble above 2 mM.

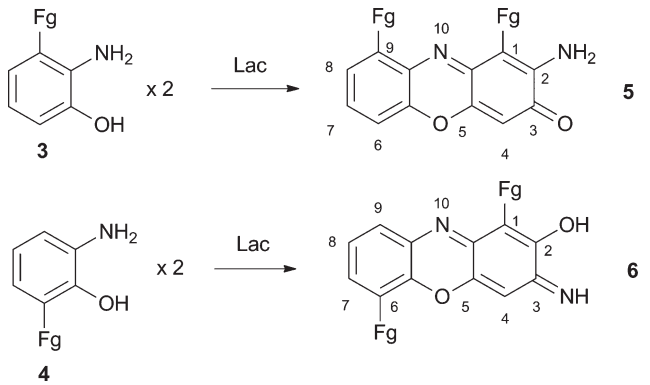

Scheme 1 Laccase-mediated synthesis of phenoxazinones. Fg = functional group responsible for tunable solubility properties. (Fg = CO_2H, SO_3H, SO_2NH_2, SO_2NHR, PO_3H_2).[12a,b,d]

obtained with laccase could be experimentally linked to an expected influence of the Hammet substituent effect.[24b,c]

Laccase-mediated oxidation of selected substrates

The results of the laccase-mediated oxidation of selected precursors with the surrogate laccase **Tv2** are given in Table 1 (column 7). The conversion yields were estimated using the HPLC-PDA analytic method previously set up to follow the biotransformations with the Bioscreen laccase **Tv1**.[12a,b,d] Recent studies show that the laccase preparation **Tv2** from a reliable commercial source behaves similarly to few natural isozymes from *Trametes versicolor*.[25] This is a practical alternative as the laccases we used previously were either uncompletely characterized (Bioscreen, **Tv1**)[26] or not yet commercially available (laccase from *Pleurotus sajor caju*).[27] In Table 1, the conversion percentages into the corresponding phenoxazinone dyes (see Scheme 1) were very similar to those collected with the Bioscreen laccase (**Tv1**) (entries 1–4). A slight decrease is observed with the more sterically hindered substrates (entries 6, 10 and 12) whereas a twofold increase is recorded for compound **4c** (entry 11). Here again, compound **4j** (entry 13) failed to give a symmetrically substituted phenoxazinone dye (general structure **6** in Scheme 1). Based on these preliminary results, pairs of precursors were selected to investigate the synthesis of non-symmetrically substituted phenoxazinones. The surrogate laccase being equally efficient for phenoxazinones synthesis, this laccase preparation (**Tv2**) was used for the remaining part of the research.

Proof of concept for the synthesis of non-symmetrical phenoxazinones

As non-symmetrical phenoxazinones have never been synthesized *in vitro* with a laccase, a "proof of concept" reaction was set up to validate our analytical method. Both the isolation and structural elucidation of the representative novel dyes were undertaken using appropriate substrates synthesized as previously described in the literature.[12b,d] Compound **3b**, which possesses a phosphorus substituent, was chosen to give reliable structural data through coupling constants analysis (J_{H-P} and J_{C-P}) in the NMR spectra. Compound **3f** was selected because it makes the LC-MS analysis easier and displays a typical fragmentation pattern in MS/MS spectra (loss of cyclohexene, −82 *m*/*z*). After 16 h of reaction (1 : 1 mixture of selected substrates, pH 6.5, 25 °C, laccase **Tv2**), HPLC analysis showed the conversion of starting materials into four phenoxazinones in a ratio of about 55/6/4/35 deduced from the percentages of area detected at 410 nm. The first and last eluted dyes were identified as **5b** (Fg = PO_3H_2) and **5f** (Fg = $SO_2NHC_6H_{11}$, Scheme 1) by comparison with references synthesized by known procedures from the literature.[12b,d] The crude reaction mixture was purified by preparative HPLC and the four phenoxazinones (**5b**, **8bf**, **7fb** and **5f**) were isolated in relative amounts corresponding roughly to the molar ratios observed by HPLC. The structural elucidation of the two novel compounds, respectively **8bf** (7.6% yield) and **7fb** (3.8%

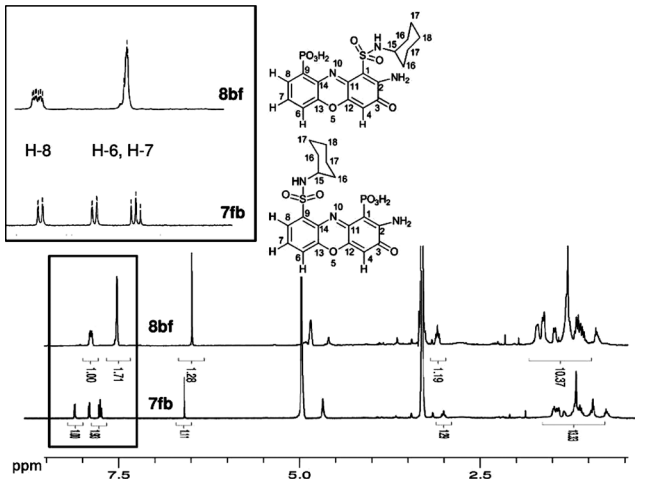

Fig. 2 From the bottom: full ^{1}H NMR spectrum of **7fb**, **8bf** followed by expansion of aromatic region of **7fb**, **8bf**. On the top right, structures of the phenoxazinones and atoms numbering for NMR attribution (see Experimental).

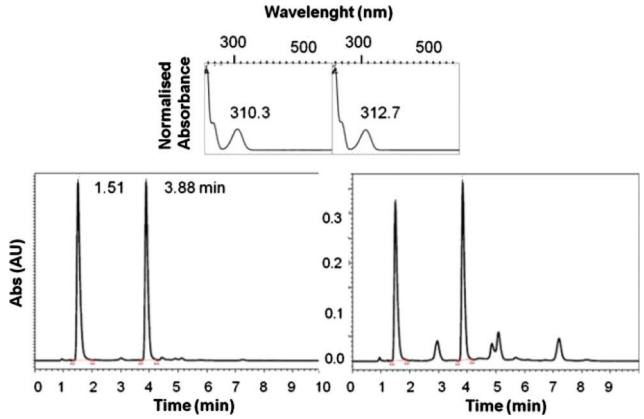

Fig. 3 HPLC-PDA analysis of the reaction of the pair of substrates **3d** and **3f** (1 mM) with the laccase **Tv2**. Top panel-left and right, **3d** and **3f** uv-vis spectra. Bottom panel-left, HPLC-UV (310 nm) analysis at T_0 (2 min), **3d** (RT = 1.51 min) and **3f** (RT = 3.88 min). Bottom panel-right, HPLC-UV (310 nm) analysis at T_3 (75 min of reaction).

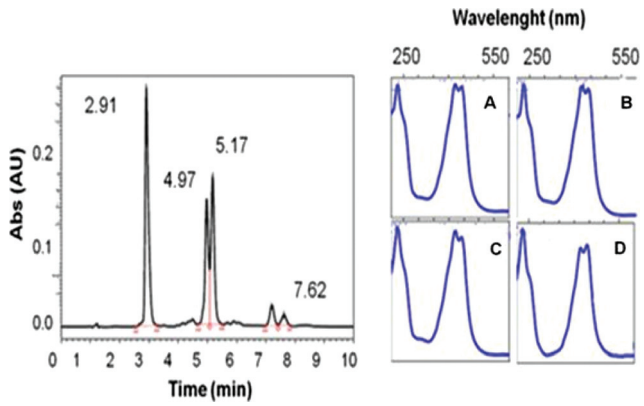

Fig. 4 HPLC-PDA analysis of the reaction of the pair of substrates **3d** and **3f** (1 mM) with the laccase **Tv2**. Panel-left, HPLC-UV (440 nm) analysis at T_3 (75 min of reaction). Panel-right, the uv-vis spectra of peak 1 (A), peak 2 (B), peak 3 (C) and peak 4 (D).

yield) were obtained from NMR analyses and high resolution mass spectra (see Experimental). In the top left panel of Fig. 2, expansions of the aromatic regions of ^{1}H NMR spectra clearly show the significant difference on the aromatic proton signals due to the coupling to the phosphorus atom. Compound **8bf** is characterized by a complex pattern (ddd) for H-8 due to the $^{3}J_{H-P}$ of 12.5 Hz whereas in compound **7fb**, ^{1}H NMR spectrum only features J_{H-H} couplings: H-8 and H-6 appear as doublet of doublets (dd), H-7 as an apparent triplet. In ^{31}P NMR, compound **8bf** is characterized by a signal at 9.5 ppm (phosphorus on an aromatic) whereas compound **7fb** appears at 12.4 ppm (phosphorus anchored to a quinone ring). A second reaction was realized with **3b** (Fg = PO_3H_2) and **3g** (Fg = $SO_2NHCH_2CO_2$-Me) which essentially gave similar HPLC elution profiles and NMR signals for compounds **8bg** (isolated in 6.8% yield) and **7gb** (isolated in 4% yield) (see ESI† for structures and atom numbering, and HPLC profiles). Here again the ratio of conversion detected by HPLC roughly corresponds to the isolated yields. It shows that even if the substrates are not significantly distinct by their oxidation potentials, oxidation is faster for **3b** and homo-dimerization appears favoured *versus* cross-dimerization (yield of **5b** about 8 to 10-times higher than **8bf** and **8bg**). The quick decrease of **3b** concentration during the reaction yields finally more of the symmetrical phenoxazinones **5f** or **5g** than the non-symmetrical **7fb** or **7fg**.

HPLC-MS/MS study of competitive laccase-mediated synthesis of phenoxazinones

The competitive experiments were then conducted systematically as above with 1 : 1 mixtures of two different aminophenol precursors, using HPLC to follow the reactions. Substrates bearing primary or secondary sulfonamide moeties, synthesized as described in precedent papers,[12a,b] were essentially chosen to ensure optimal retention times and separations on the HPLC column. The samples were analyzed by HPLC-PDA (retention times given in the ESI†) and these non-symmetrically substituted phenoxazinones were further unambiguously identify by HPLC-MS/MS as the analytic method (full identification data in ESI†).‡ The relative rates of conversion were estimated from the area decreases and increases of the respective precursors and phenoxazinones in the first 75 min of reaction with laccase (Table 2). This process is exemplified in Figs 3 and 4 with the pair of precursors **3f** and **3d**; the detection of substrates (aminophenols) and products (phenoxazinones) is made respectively at 310 and 440 nm. Finally, compound **4j** was included in the set to determine by HPLC-MS/MS if it is oxidized or acts only as a nucleophilic partner.

After 75 min, a faster consumption of **3d** *versus* **3f** is observed along with the appearance of the corresponding phenoxazinones **5d**, **5f**, **7df** and **8fd** featuring the specific λ_{max} at 220–240 nm and 420–440 nm (see Fig. 4 and Scheme 2). From the four peaks detected at 440 nm, peak 1 and 4 correspond, respectively, to the known dyes **5d** and **5f** (see Scheme 1).[12b] Peaks 2 and 3 correspond to novel phenoxazinones (**8df** and **7fd**, see ESI† for identification) well distinct from the symmetrical dyes (**5d**, **5f**)

Table 2 Relative area variations for the precursors and phenoxazinones[a]

	ΔArea $(A_{T0} - A_{T3})/A_{T0}$		ΔArea $(A_{T3} - A_{T1})/A_{T3}$			
Entry	Δ*A*-(cmpd)	Δ*A*-(cmpd)	Δ*A* (dye 1)	Δ*A* (dye 2)	Δ*A* (dye 3)	Δ*A* (dye 4)
1	0.34-(**3f**)	0.43-(**3d**)	0.55-(**5d**)	0.54-(**8df**)	0.48-(**7fd**)	0.32-(**5f**)
2	0.30-(**3f**)	Na-(**3c**)	0.23-(**5c**)	0.28-(**8cf**)	0.28-(**7fc**)	0.50-(**5f**)
3	0.33-(**3f**)	0.30-(**3j**)	0.19-(**5j**)	0.13-(**8jf**)	0.07-(**7fj**)	0.34-(**5f**)
4	0.05-(**3f**)	0.40-(**4f**)	0.02-(**10ff**)	0.52-(**9ff**)	0.38-(**6f**)	0.12-(**5f**)
5	0.15-(**3d**)	0.26-(**4f**)	Nd-(**5d**)	0.46-(**9df**)	0.03-(**10fd**)	0.42-(**6f**)

[a] Precursors (1 mM) were mixed with laccase **Tv2** (100 UL^{-1}) in 1 mL of 0.2 M ammonium acetate buffer at 25 °C. Area for each precursor (310 nm) and dyes (440 nm) were measured at T_0 (2 min), T_1 (25 min), T_2 (50 min) and T_3 (75 min). Na = not available as **3c** was transformed in the first 25 min. Nd = not determined as the small amount of **5d** detected at T_1 did not increase further.

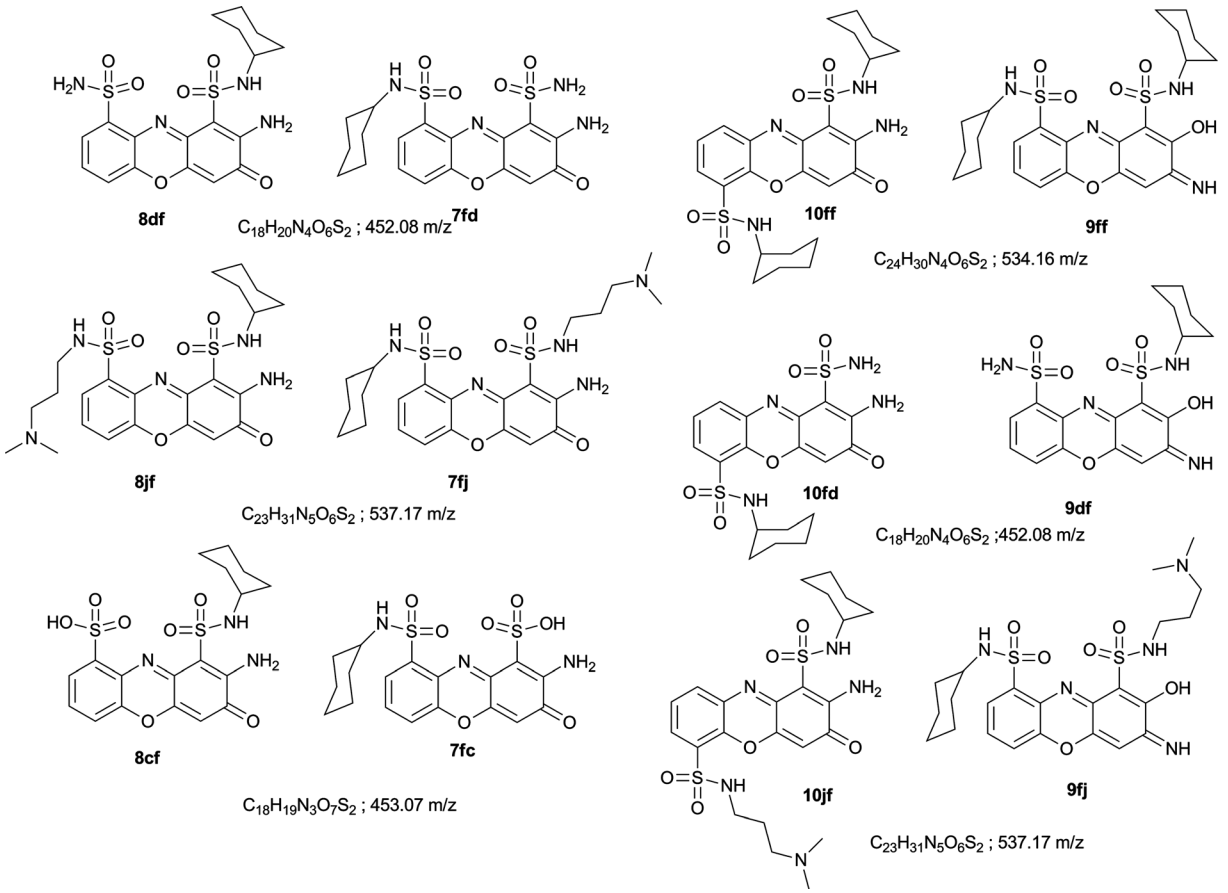

Scheme 2 Structures of non-symmetrically substituted phenoxazinones produced by oxidative cross-coupling reactions and identified from HPLC-PDA and HPLC-MS/MS analyses (see ESI† for full description of identification data).

and close to each other in the elution profile (see Scheme 2, Figs 3 and 4). Results of the HPLC-MS/MS analysis in the identification process for the pair **3f–3d** (entry 1, Table 2) are exemplified in Fig. 5 (fully described in ESI†).

The relative rates of conversion for all precursors and the distinct heterocyclic dyes are presented in Table 2. Entry 1 of Table 2 shows that the conversion of **3d** into **5d** is faster than **3f** into **5f** in the earlier hours of reaction. Both independent laccase-mediated syntheses of **5d** and **5f** (Table 1, entries 4 and 6) and also the oxidation potential of **3d** and **3f** are very similar. Yet a greater efficiency of the biocatalyst for **3d** *versus* **3f** is observed here. Entry 2 shows again that despite being close regarding their oxidation potential, a faster oxidation rate for **3c** *versus* **3f** is still observed. Interestingly, the appearance of **5f** is the most important whereas all the three other dyes (**5c**, **7fc** and **8cf**) are formed in lower proportions. The compound **3c** may be a poor nucleophile whereas **3f** is a good one that reacts quickly with both the oxidized **3c** and **3f** (Scheme 3). In entry 3, a similar rate of conversion is observed for **3f** and **3j** (see Table 1, entries 6 and 10). Yet, the rate of formation for the dyes 1–4 differs significantly, descending from **5f–5j–8jf** to finally **7fj**. It suggests a preference for **3f** reacting as a nucleophilic partner upon its own oxidized intermediate (Scheme 3). This may be related to a hydrophobic effect of the substrate since **3j** is more polar around

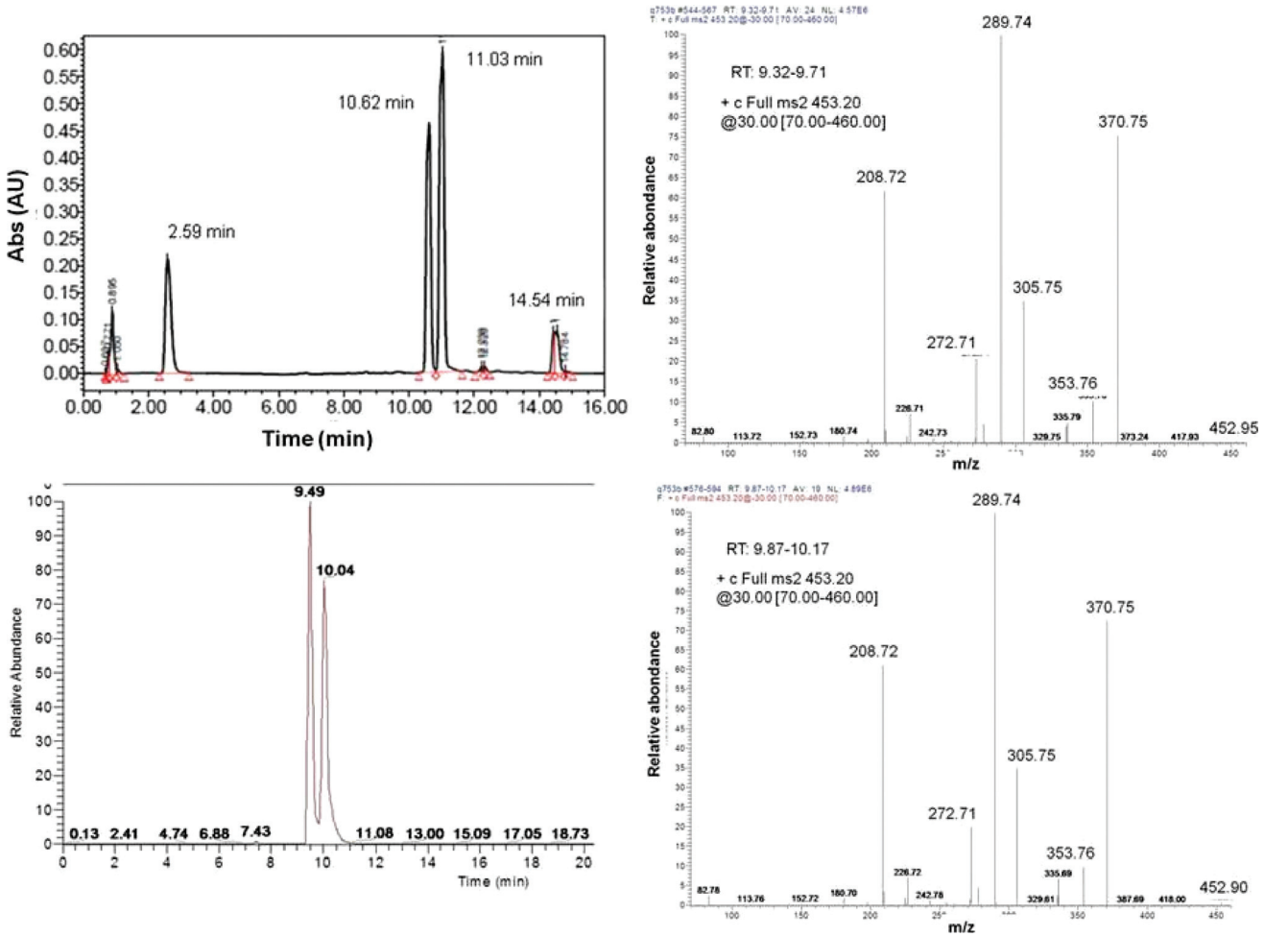

Fig. 5 HPLC-PDA analysis of the reaction of the pair of substrates **3d** and **3f** (1 mM) with the laccase **Tv2** (100 UL^{-1}) at 25 °C in 0.2 M ammonium acetate buffer (pH 6). Top panel-left, HPLC-UV (440 nm) analysis after 24 h of reaction. Peak 1 (RT = 2.59 min) is **5d**, peak 2 (RT = 10.62 min) and peak 3 (RT = 11.06 min) are **8df** and **7fd** (Fg1 = SO_2NH-cyclohexyl, Fg1′ = SO_2NH_2). Analytic condition with XTerra (2.1 × 50 mm, 2.5 µm), flow rate = 0.2 mL min^{-1}. Bottom panel-left, HPLC-MS-MS (ESI positive mode, *m*/*z* 453) analysis of the sample after 24 h of reactions. Divert valve was set between 2.1 and 16.9 min, peak 2 eluted at 9.49 min and peak 3 at 10.04 min. Top panel-right, mass spectrum of peak 2 (9.49 min). Bottom panel-right, mass spectrum of peak 3 (10.04 min). (see ESI† for full identification data).

pH 6 due to its protonated tertiary amino-group. Entry 4 is interesting as the conversion of **4f** is impressively quicker than **3f** and the formation of **6f** is also faster than **5f**. The most peculiar result is the significant larger proportion of only one non-symmetrically substituted dye (**9ff**). This heterodimeric dye corresponds to the residual nucleophilic **3f** reacting with the larger proportion of oxidized **4f** (Scheme 3). Finally, entry 5 shows that **4f** is converted more quickly than **3d**. Again, two dyes are significantly produced in larger proportions. A hydrophobic effect may explain the larger quantity of **6f** whereas the major decrease of **3d** is related to the nucleophilic addition of **3d** upon the oxidized **4f**. From these results, an overall reactivity scale going from **3c**~**4f**~**3b**–**3d**–**3j**–**3f** may be proposed. It can be correlated to the kinetic data obtained previously (**4f**–**3d**–**3c**–**3j** from Table 1, column 8). In addition, by mixing **3f** and the previously inert **4j**, a major new peak was detected in both HPLC-PDA and HPLC-MS. The corresponding ion with *m*/*z* of 538 $[M + H]^+$ ($C_{23}H_{31}N_5O_6S_2$) gave in tandem mass spectrometry the typical fragmentation along with a loss of neutral fragment of *m*/*z* 45 ($HNMe_2$) indicative of the tertiary amino group. A second compound with identical mass *m*/*z* 538 was detected in a tiny amount. The same fragmentation pattern was observed. This suggests that the major compound arises from laccase-mediated oxidation of **3f** and subsequent 1,4-addition of native **4j** (Scheme 2, phenoxazinone **10jf**). The very minor compound would arise from auto-oxidation of **4j** and subsequent 1,4-addition of native **3f** (Scheme 2, phenoxazinone **9fj**). The redox-properties and apparent affinities for the enzyme seem to be reflected in the formation of the phenoxazinones. Interestingly Cambria *et al.* published in 2010 a report about a laccase from *Rigidiporus lignosus*, highly similar to the inducible laccase from *Trametes versicolor* and presenting similar kinetic properties.[28] This suggests that a comparison between kinetic data collected with laccases from *Pleurotus sajor caju* and **Tv2** holds pertaining information.[12b] The experimental results indicate that non-symmetrically substituted phenoxazinones are indeed formed in various proportions most probably depending on the redox-properties of the precursors and their relative affinity for the enzyme. We have proven that compound **4j** acts as an efficient nucleophilic partner and is weakly auto-oxidized *in situ*.

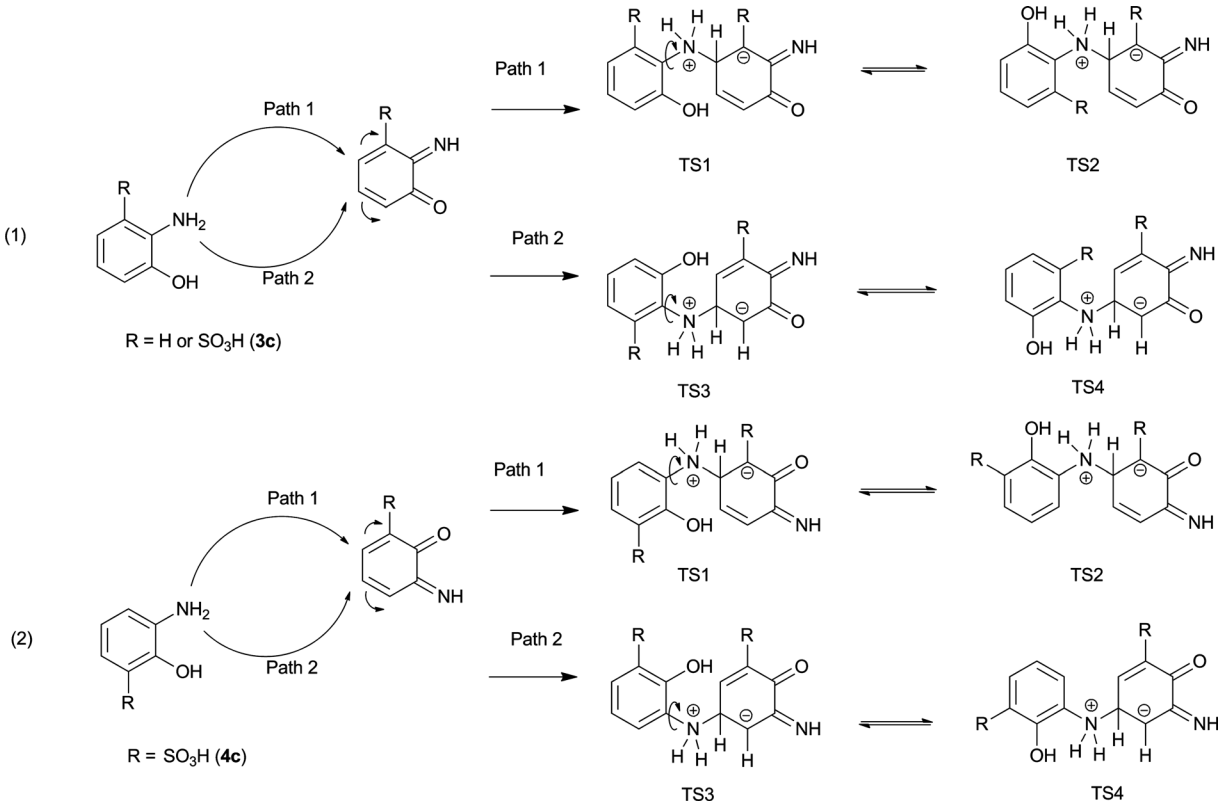

Scheme 3 Proposed pathways for the intermolecular 1,4-addition of *o*-aminophenol substrates onto imino-quinone intermediates (first Michael addition step).

Although it seems inert towards laccase-mediated oxidation, recently **4j** was successfully oxidized into phenoxazinone by tyrosinase.[29]

Theoretical study of the regioselectivity of the 1,4-addition

The addition of the native *o*-aminophenol on the neutral imiquinone intermediate can be done following two paths depending on the regioselectivity of the Michael addition. Each of these adducts can adopt two conformations of the phenol (Scheme 3, paths 1 and 2). This first reaction step has been investigated by the location of the transition state (TS) structures at two computational levels using RHF/6-31+G and B3LYP/6-31+G(d) energy functions (see ESI† for details). It can be noted that the partial inclusion of the correlation energy with B3LYP and the additional polarization functions to the double ζ basis set including diffuse functions do not modify the relative energies of the TS (Table 3 and details in ESI†). In each case, the imaginary frequency is associated to the exchange of the H between the NH

Table 3 *Ab initio* and DFT relative energies (kcal mol^{-1}) for transition states[a]

Entry	Substrate	Transition state (TS)	RHF/6-31+G (ΔE)	B3LYP/6-31+G(d) (ΔE)	B3LYP/6-31+G(d) (ΔG)
1	***o*-aminophenol**	TS1	77.293	55.344	66.796
	R = H	TS2	72.889	57.787	69.061
		TS3	61.251	45.300	57.378
		TS4	64.754	47.574	59.670
2	**3c**	TS1	58.515	35.659	48.704
		TS2	49.953	40.851	53.178
		TS3	69.060	51.373	62.835
		TS4	60.735	43.401	56.287
3	**4c**	TS1	50.394	39.285	52.377
		TS2	52.352	41.274	55.493
		TS3	80.126	60.936	72.078
		TS4	85.572	Na	Na

[a] See Scheme 3 for the outline of the reaction paths involving the different transition states. Reactants are local minima energy obtained from RHF/6-31+G or B3LYP/6-31+G(d) optimized geometries. ΔE and ΔG (kcal mol^{-1}) are defined with respect to the sum of the lowest energies RHF/6-31+G or B3LYP/6-31+G(d) for the reactants. Na = not located equilibrium structure

group and the proximal carbon defining a pseudo four-membered ring (see ESI† for representative description of equilibrium structures). The calculation results are summarized in Table 3. With R = H, path 2 is energetically more favorable than path 1, the relative energies of the two conformers lying in a 2–3 kcal mole^{-1} range. The same type of calculations has been performed with R = SO_3H at the two positions in **3c** and **4c**. Remarkably, in accordance with the experimental data, path 1 is energetically less demanding than path 2. For **4c**, the TS4 structure can be trapped only at the RHF level. No corresponding equilibrium structure can be located with the B3LYP function. Thus, the favoured addition corresponds to the nucleophilic attack on the β-carbon *vs.* the electron-withdrawing Fg substituent, in all cases. This leads to zwitterionic intermediates with the negative charge stabilized by Fg (see ESI† for representative equilibrium structure).[30]

Hypothesis for the laccase-mediated synthesis of phenoxazinones

Consistently with our experimental results, we propose a mechanistic pathway for the production of substituted phenoxazinones using laccase as catalyst. Our mechanistic proposal is adapted from Barry *et al.* regarding the actinomycin synthesis catalyzed by phenoxazinone synthase.[8] Here, the heterocycle is produced in the early hours of the reaction and the residual part of the native precursor is still present in significant amounts (HPLC analyses). This fact points to a non-electrophilic mechanism in contrast to the formation of grixazone.[5a] The overall process is depicted in Scheme 4. Briefly, the first two steps are the ones revisited with our hypothesis. Depending on its affinity for the enzyme, the *o*-aminophenol precursor is quickly oxidized through two successive one-electron oxidations. Alternatively a single laccase-mediated one-electron oxidation could produce the anthranilyl radical which could undergo a further reaction.[9] Indeed cinnabarinic acid (Fg = CO_2H, formula **5** in Scheme 1) is also produced in reactions involving radicals and molecular oxygen.[31–35] Yet, our suggestion that the laccase could directly generate a quinone intermediate, in accordance with studies on oxidase model,[33] is compatible with our experimental results in terms of selectivity and isolated yields. Oxidation at the laccase Cu-site T1 is governed by the Marcus outer sphere mechanism,[19b] and the rate limiting step, facilitated through hydrogen bonding, is the extraction of electrons from the substrate.[19a] The transient intermediate iminoquinone flows out the binding cavity and reacts with a nucleophilic partner in the bulk of the solution. 2-amino-3-oxo-3*H*-phenoxazine-8-sulfonic acid was reported to be produced by a laccase *in vitro* without detection of any radical intermediate by the EPR technique;[12c] this adds some weight to our proposal. Indeed, the same technique successfully identified radical intermediates in several related reactions.[36] The second step, *i.e.* the first 1,4-conjugated addition, would most probably take place in the bulk of the solution and the regiochemistry is secured by the rules governing the Michael addition. From the isolated yields in the "proof of concept" reactions, the major path of conversion corresponds to the addition of the best nucleophiles present in solution *i.e.* the aminophenols. Yet side reactions could not be ruled out and by-products or intermediates were indeed observed in preparative HPLC (see ESI†). Nevertheless these results are similar to those obtained with substituted catechols either in presence of laccase, or by electrochemical oxidation.[13,36] The subsequent steps of oxidation, intramolecular 1,4-conjugated addition and final oxidation are supposed to be identical to those previously described for the phenoxazinone synthase.

Docking of selected substrates

One of the substrates (**4j**) failed to be transformed by the laccase whereas it performed well as a nucleophilic partner. We envision that a poor fitting of the substrate in the binding cavity could be a reason for this behavior. At the pH of our experiments (pH of 6.5 for 0.2 M ammonium acetate), Asp206 is mostly deprotonated and aromatic substrates with –OH and –NH_2 groups are recognized and dragged inside the cavity by hydrogen bonding with Asp206.[19b,22,28] The known structure of *Trametes versicolor* enzyme complexed with *p*-xylidine (1kya) is regularly used as a benchmark for docking studies of small molecules.[19,28,37] Furthermore, the Bioscreen laccase has been experimentally related to the inducible isozyme form (Lac2) from *Trametes versicolor*[26] whereas the major constituent of the commercial laccase preparation **Tv2** seems related to the major isozyme (Lac1) of *Trametes versicolor*.[25a] This prompts us to investigate by simple rigid docking the steric factors which could possibly prevent the oxidation of **4j** by the laccase (Fig. 6). Before

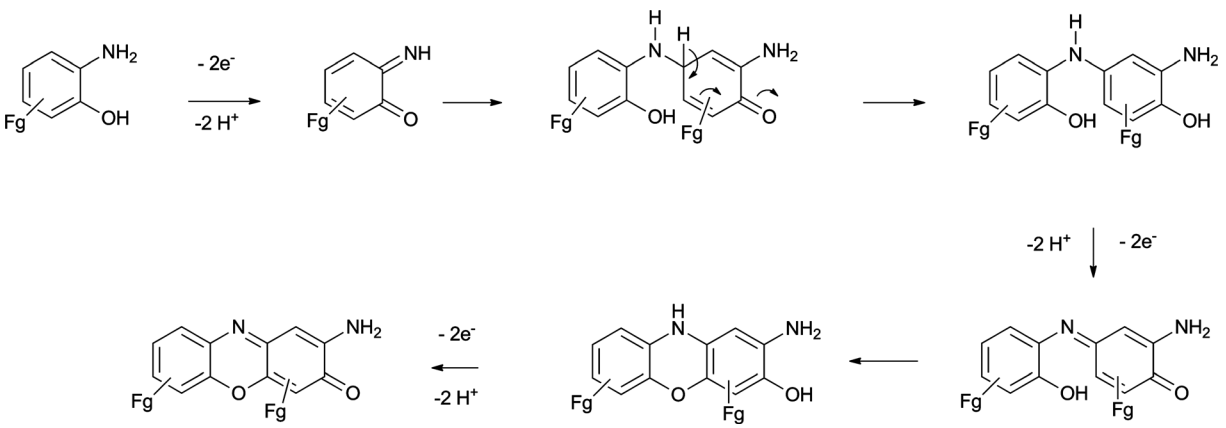

Scheme 4 Mechanistic pathway for the synthesis of symmetrically and non-symmetrically substituted phenoxazinones from *o*-aminophenol substrates.

Table 4 Docking of selected substrates with Molegro virtual docker[a]

Entry	Ligand	Mol dock score of docked poses (Productive)[b]				
		Pose-1	Pose-2	Pose-3	Pose-4	Pose-5
1	***p*-xyd**			−52.5 (Y)		
2	**3c**	−48.3 (N)	−52.2 (Y)	−54.1 (Y)	−53.6 (Y)	—
3	**3f**	−48.3 (N)	−31.3 (N)	−11.6 (N)	−36.9 (Y)	−71.7 (N)
4	**3j**	−47.2 (N)	−53.1 (N)	−50.8 (M)	−41.5 (M)	−47.5 (Y)
5	**4c**	−54.8 (M)	−51.5 (M)	−43.1 (Y)	−52.8 (M)	—
6	**4f**	−40.1 (N)	−8.2 (N)	−27.5 (N)	−72.4 (N)	−22.8 (Y)
7	**4j**	−79.3 (M)	−78.2 (N)	−72.3 (M)	−57.3 (N)	−67.0 (N)

[a] Productive docking: Y = Yes (–OH group is directed towards Asp206 and His458 with a positioning at, or almost at, the expected hydrogen bonding position); M = Medium (–NH_2 group is directed towards Asp206 and His458 with a positioning at the expected hydrogen bonding position); N = No (= sulfonamide moiety is either hydrogen bonded or pointing towards the inner of the cavity). See ESI† for complete listing of docked poses. [b] The total MolDock Score energy (arbitrary units) is the sum of internal ligand energies, protein interaction energies and soft penalties. See ref. 39 for further details.

docking, the conformations of selected substrates were energy minimized. From the X-ray crystal structure (PDB ID-1kya) the receptor pocket was prepared with the Molegro Virtual Docker program.[38,39] The software has a procedure allowing to create a "template docking environment". Briefly *p*-xylidine is taken as the reference ligand; a cavity is detected around the ligand in which steric factors and hydrogen bonds are identified along with a preferential positioning of the aromatic ring (see ESI†). Rotating/flexible bonds are identified for each ligand while the receptor cavity is kept rigid. From there, a scoring function (Moldock score)[39] associated to the total energy of the system is given to rank the different poses observed. As a reference ligand is used, a RMSD constraint <1 Å (RMS deviation) is also taken into account. For each substrate 10 runs (1500 iterative searches) are undertaken from which only the 5 best docked conformations are kept. In Table 4 we present the docked poses with an orientation corresponding to either the aromatic –OH or –NH_2 group yielding productive hydrogen-bonds. The docked poses featuring non productive hydrogen-bonds, with the sulfonate/sulfonamide moeity, are also given. To validate the procedure, *p*-xylidine is docked into the receptor cavity with a score taken as the reference (see Table 4, entry 1). It can be observed that compounds **3c**, **3f** and **3j** gave at least one productive docking with the –OH group forming hydrogen bonds with Asp206 and His458. As expected, the smaller **3c** gave the highest score with multiple optimal docking whereas **3f** and **3j** only gave one productive conformation with the side chains pointing towards the outside of the cavity. For **4c**, one conformation featured the –OH group hydrogen-bonded to His458 whereas the sulfonic group pointed partially into the cavity. An electrostatic repulsion could impair the efficiency of this binding mode. The other docked conformations showed the sulfonate pointing outside the cavity with the –NH_2 group hydrogen-bonded. One conformation for **4f** also featured the –OH group involved in hydrogen bonding whereas for **4j**, only one conformation with –NH_2 and –OH groups pointing into the inner part of the cavity was found. In this docked pose, the –NH_2 group is at a distance of about 3 Å from both His458 and Asp206. Further ligand energy minimization could not improve the positioning of **4j**. Docked pose 1 provided the –OH group in the inner cavity albeit with a folding of the sulfonamide function towards the aspartate and this aromatic –OH group. The absence of a docked conformation featuring the aromatic –OH group bonded to Asp206 and His458, is not *per se* a proof that the laccase is not able to process **4j**, but reinforces our experimental observations.

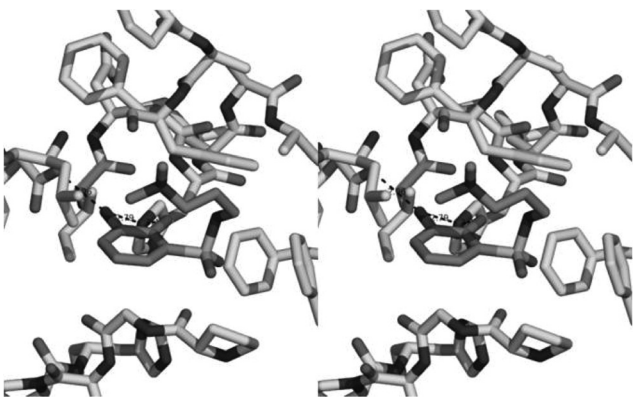

Fig. 6 A stereo view of docked pose 3 of **4j** obtained with Virtual Molegro Docker into the binding cavity. View elaborated with Pymol software.[40] The –NH_2 group is at the expected position for the hydrogen bonding with Asp206 and His458.

Conclusion

Several non-symmetrically substituted phenoxazinones were isolated and identified for the first time in laccase-mediated coupling reactions of *o*-aminophenols *in vitro*. Taking advantage of the previous isolation and structural characterization of symmetrically substituted phenoxazinones, we have successfully mimicked a natural transformation using mixtures of structurally-close substrates. Redox properties were assessed and it was shown that a careful selection of pairs of substrates could lead to some control of the process by favoring one heterocycle *versus* another. A qualitative correlation between both steric and redox properties became apparent through the rates of conversion. The chemoselectivity and regioselectivity observed could be explained through DFT calculations, supporting our revisited mechanism. We propose that the laccase-mediated oxidation of a

given *o*-aminophenol is a formal two-electron oxidation that generates directly a short lived iminoquinone intermediate. This highly electrophilic species then reacts with a nucleophilic partner (i.e the same *o*-aminophenol or another similar substrate) in the bulk of the solution following the chemical rules governing the classical 1,4-conjugated addition (Michael addition). One compound (**4j**), inert towards laccase-mediated transformation, could still yield a non-symmetrically substituted phenoxazinone by acting as nucleophile *versus* another processable *o*-aminophenol. This observation strongly supports our original hypothesis that the key-step of the oxidative dimerization, namely the first Michael addition, proceeds outside the laccase cavity.

Experimental Details

Reagents and analyses of synthesized and isolated compounds

All aminophenols and aminophenoxazinones compounds were synthesized as previously described[12a,b,d] except 3-hydroxyanthranilic acid, which is commercially available (Aldrich). All the reagents and solvents used were of analytical grade and obtained from either Acros or Aldrich company. Commercial preparation of laccase **Tv2** from *Trametes versicolor* was obtained from Aldrich (38429 or 53739). The HPLC-PDA semi-preparative system consisted of Waters Alliance 2699 separation module, Waters 2998 photodiode array detector and Waters Fraction collector III (Waters, Milford, Massachussets, USA). Analytical separations were performed with Waters XBridge™ C18 column (4.6 × 50 mm, 2.5 µm) equipped with a precolumn at 25 °C. Detection was performed at 410/440 nm and on-line uv-visible scans were performed. Semi-preparative separations were performed with Waters Xbridge™ Prep C18 column (10 × 100 mm, 5 µm) equipped with a precolumn at 25 °C. The mobile phase was water, ammonium acetate 50 mM/acetonitrile (5%) and acetonitrile. A linear gradient (curve 6) was applied from 0/90/10 to 0/10/90 for 7.5 min after 0.5 min at initial conditions and before 2 min at final conditions (for **3b** and **3f**). A linear gradient (curve 6) was applied from 10/80/10 to 10/10/80 for 7.5 min after 0.5 min at initial conditions and before 2 min at final conditions (for **3b** and **3g**). The flow rate was set at 1.2 mL min^{-1} for the analytical method (10 µL injection). For preparative separations, the flow rate was set at 4 mL min^{-1}. A linear gradient (curve 6) was applied from 10/80/10 to 10/10/80 for 9.5 min after 0.5 min at initial conditions and before 4 min at final conditions (100 µL injection). An equilibration time of 4 min was used between successive injections. ^{1}H, ^{31}P and ^{13}C NMR spectra were recorded with a Bruker Avance 500 spectrometer. Spectra were obtained in methanol-d_4 with a small addition of D_2O for **8bg**. Chemical shifts are reported in ppm relative to TMS or H_3PO_4 85% for ^{31}P NMR. Low resolution mass spectra were acquired using a Thermo Finnigan LCQ spectrometer either in positive or negative mode ESI. High Resolution Mass Spetrometry (HRMS) analyses using ESI were performed at the University College of London (UK).

Laccase-mediated chemical synthesis: general procedure

A solution of 1 equivalent of each aminophenol in methanol (3 mL, 0.055 mmol for **3b** and **3f**, 0.25 mmol for **3b** and **3g**) was added to a stirred solution (57 mL) of 0.2 M of ammonium acetate at 25 °C. The reaction was started by adding a solution (0.2 mL) of Laccase (1.5 mg mL^{-1}, *Trametes versicolor*, Aldrich 53739, 20 Umg^{-1}). HPLC analysis showed the total consumption of the starting materials after 16 h. The solution was then freeze-dried and the residual solid was dissolved in methanol (1.2 mL), filtered on a PTFE syringe filter (SFPF02213-C1, ROCC) and added to water (1.2 mL) before being filtered again. The filtrate was directly used for purification by preparative HPLC. The filters were rinsed several times with water and methanol respectively. The respective washing solutions were concentrated and dried under vacuo.

2-Amino-3-oxo-3*H*-phenoxazine-9-phosphonic acid-1-sulfonic acid cyclohexylamide (8bf)

0.055 mmol of substrates (total mass of 27 mg) were engaged and 30 mg of crude product were obtained. Concentrated washing solutions (mainly symmetrical dyes **5b** and **5f**) gave respectively 7 and 2 mg. 18 mg of the crude were purified by HPLC-Prep yielding four fractions which, respectively, correspond to **5b** (5.8 mg), **8bf** (2 mg), **7fb** (1 mg) and **5f** (8.5 mg). The title product was isolated as an orange solid. Yield: 7.6% (2 mg). RT: 3.37 (analytical) and 5.09 min (preparative). MW: $C_{18}H_{20}N_3O_7PS$, 453.40 g mol^{-1}. ^{1}H NMR (500 MHz, methanol-d_4) δ = 7.88 (1H, ddd, J_{H-H} = 5.5, 3.0 and J_{H-P} = 12.5 Hz, H-8), 7.53–7.51 (2H, m, H-7 and H-6), 6.48 (1H, s, H-4), 3.09 (1H, tt, J_{H-H} = 3.9, 11.3 Hz, H-15), 1.71 (2H, m, Ha-16), 1.62 (2H, m, He-16), 1.49–1.05 (6H, m, H-17,18) ppm. ^{31}P NMR (202.4 MHz) δ = 9.54 (Ar–PO_3H_2) ppm. ^{13}C NMR (125 MHz, BB-decoupling (48 h), missing C11,C13,C14) δ = 179.6 (C3), 151.2 (C12), 147.7, (C2), 134.4 (C9, J_{C-P} = 162 Hz), 130.6 (C8, J_{C-P} = 14.5 Hz), 129.6 (C7, J_{C-P} = 6.7 Hz), 118.6 (C6), 105.3 (C4), 55.0 (C15), 34.2 (C16), 30.7 (C18), 26.2 (C17) ppm (see Fig. 2 for atoms numbering). UV/Vis (ammonium acetate 10 mM), λ_{max} = 231, 430–439 nm. MS (ESI) *m/z* (%): 452.43 $[M - H]^-$ (100), 474.37 $[M-2H + Na]^-$ (70), 434.2 (25); MS^2 of 452.3 *m/z* yields 434.3 [−18] and 370.38 [−82, $-C_6H_{10}$] *m/z*. HRMS (ESI negative mode): clcd = 452.0681 for $C_{18}H_{19}N_3O_7PS$; found 452.0698.

2-Amino-3-oxo-3*H*-phenoxazine-9- sulfonic acid cyclohexylamide-1-phosphonic acid (7fb)

The title product was isolated as a red solid. Yield: 3.8% (1 mg). RT: 3.65 (analytical) and 5.73 min (preparative). MW: $C_{18}H_{20}N_3O_7PS$, 453.40 g mol^{-1}. ^{1}H NMR (500 MHz, methanol-d_4) δ = 7.85 (1H, dd, J_{H-H} = 7.7, 1.1 Hz, H-8), 7.66 (1H, dd, J_{H-H} = 8.3, 1.1 Hz, H-6), 7.52 (1H, t, J_{H-H} = 8.0 Hz, H-7), 6.41 (1H, s, H-4), 3.03 (1H, tt, J_{H-H} = 3.9, 11.2 Hz, H-15), 1.62–1.48 (4H, m, H-16), 1.49–1.05 (6H, m, H-17,18) ppm. ^{31}P NMR (202.4 MHz) δ = 12.49 (PO_3H_2) ppm. ^{13}C NMR (125 MHz, BB-decoupling (24 h), missing C1, C11 and J_{C-P}) δ = 182.0 (C3), 151.4 (C12), 149.8 (C2), 143.6 (C13), 138.7 (C9), 131.1 (C14), 128.4 (C7), 125.6 (C8), 121.2 (C6), 105.6 (C4), 55.0 (C15), 34.3 (C16), 30.7 (C18), 26.3 & 26.1 (C17) ppm (see Fig. 2 for atoms numbering). UV/Vis (ammonium acetate 10 mM), λ_{max} = 223, 423–440 nm. MS (ESI) *m/z* (%): 452.38

$[M - H]^-$ (100), 474.43 $[M-2H + Na]^-$ (70); MS^2 of 452.3 *m/z* yields 434.3 [−18] and 370.51 [−82, $-C_6H_{10}$] *m/z*, MS^2 of 454.40 [M+H] *m/z* yields 371.95 [−82, $-C_6H_{10}$] *m/z*. HRMS (ESI negative mode): clcd = 452.0681 for $C_{18}H_{19}N_3O_7PS$; found 452.0704.

{2-amino-1-[(2-methoxy-2-oxoethyl)sulfamoyl]-3-oxo-3*H*-phenoxazin-9-yl}phosphonic acid (8bg)

0.25 mmol of substrates (total mass of 114 mg) were engaged and 117 mg of crude product were obtained after freeze-drying. 90 mg of the crude were purified by HPLC-Prep yielding four fractions which respectively correspond to **5b** (48.7 mg), **8bf** (8 mg), **7fb** (5 mg) and **5f** (13.2 mg). The title product was isolated as an orange solid. Yield: 6.8% (8 mg). RT: 2.91 (analytical) and 3.69 min (preparative). MW: $C_{15}H_{14}N_3O_9PS$, 443.30 g mol^{-1}. ^1H NMR (500 MHz, methanol-d_4/D_2O (9/1)) δ = 7.87 (1H, ddd, J_{H-H} = 5.1, 3.5 and J_{H-P} = 12.6 Hz, H-8), 7.55–7.53 (2H, m, H-7 & H-6), 6.49 (1H, s, H-4), 3.83 (2H, s, H-15), 3.55 (3H, s, H-17) ppm. ^{31}P NMR (202.4 MHz) δ = 9.49 (Ar–PO_3H_2) ppm. ^{13}C NMR (125 MHz, BB-decoupling (24 h)) δ = 179.6 (C3), 171.6 (C16), 151.5 (C12), 147.8 (C11) 144.3 (C2), 143.6 (C13, J_{C-P} = 12.6 Hz), 137.7 (J_{C-P} = 171.6 Hz, C9), 134 (J_{C-P} = 5.6 Hz, C14), 130.7 (J_{C-P} = 15.1 Hz, C7), 130.0 (C1), 129.6 (J_{C-P} = 6.6 Hz, C8), 118.8 (J_{C-P} = 2.3 Hz, C6), 105.4 (C4), 52.6 (C17), 44.9 (C15) ppm (see ESI† for atoms numbering). UV/Vis (ammonium acetate 10 mM), λ_{max} = 231, 438 nm. MS (ESI) *m/z* (%): 442.23 $[M - H]^-$ (50), 464.15 $[M-2H + Na]^-$ (48), 291.3 (100); MS^2 of 442.3 *m/z* yields 355.09 and 291.34 *m/z*. HRMS (ESI negative mode): clcd = 442.0110 for $C_{15}H_{13}N_3O_9PS$; found 442.0132.

{2-amino-9-[(2-methoxy-2-oxoethyl)sulfamoyl]-3-oxo-3*H*-phenoxazin-1-yl}phosphonic acid (7gb)

The title product was isolated as an orange solid. Yield: 4% (5 mg). RT: 3.23 (analytical) and 4.09 min (preparative). MW: $C_{15}H_{14}N_3O_9PS$, 443.30 g mol^{-1}. ^1H NMR (500 MHz, methanol-d_4) δ = 7.95 (1H, dd, J_{H-H} = 7.4, 1.4 Hz, H-8), 7.57 (1H, dd, J_{H-H} = 8.3, 1.4 Hz, H-6), 7.53 (1H, apparent t, J_{H-H} = 7.4 Hz, H-7), 6.47 (1H, s, H-4), 3.80 (2H, s, H-15), 3.58 (3H, s, H-17) ppm. ^{31}P NMR (202.4 MHz) δ = 12.75 (PO_3H_2) ppm. ^{13}C NMR (125 MHz, BB-decoupling (24 h), missing C1 and J_{C-P}) δ =.179.5 (C3), 171.7 (C16), 150.8 (C12), 148.1 (C11), 145.1 (C2), 143.7 (C13), 142.7 (C14), 130.8 (C9), 129.9 (C7), 125.6 (C8), 119.5 (C6), 105.0 (C4), 52.4 (C17), 45.0 (C15) ppm (see ESI† for atoms numbering). UV/Vis (ammonium acetate 10 mM), λ_{max} = 231, 430–439 nm. MS (ESI) *m/z* (%): 442.27 $[M - H]^-$ (70), 464.15 $[M-2H + Na]^-$ (100), 291.4 (100); MS^2 of 442.3 *m/z* yields 355.27 and 291.38 *m/z*. HRMS (ESI negative mode): clcd = 442.0110 for $C_{15}H_{13}N_3O_9PS$; found 442.0128

Electrochemical instrumentation and measurements

Compounds were dissolved in a solution of $N(nBu)_4BF_4$ 100 mM in DMF (10 mL) to reach a final concentration of 1 mM. Freshly made solutions were used directly. Cyclic voltammograms (CVs) were recorded on a potentiostat EG&G model 283. Glassy carbon working electrode/Platinum foil counter electrode/Reference electrode: Ag/AgCl in EtOH sat LiCl. CVs were recorded in triplicate at a scan rate of 150 mV s^{-1} with a potential of −0.5 to 1.8 V. Oxidation potentials were obtained from peak of maximum current intensity at the end of the oxidation wave. Current polarity was defined according to the EU convention.

High-pressure liquid chromatography-PDA instrumentation

System 1 used for Table 1 **and** Table 2: the HPLC-PDA system consisted of Waters Alliance 2699 separation module, Waters 2998 photodiode array detector (Waters, Milford, Massachussets, USA). Analytical separation were performed with Waters XTerraMsC18 column (4.6 × 100 mm, 5 µm) at 25 °C. Detection was performed at 310/440 nm and on-line uv-visible scans were performed. Flow rate was 1 mL min^{-1}. Injection volume was of 10 µL. The mobile phase was water/formic acid (0.1%) and acetonitrile/formic acid (0.1%). A hyperbolic gradient (curve 2) was applied from 75/25 to 25/75 in 20 min before applying a hyperbolic gradient (5 min) to the initial conditions.

System 2 used for Table 3: the HPLC-PDA system consisted of Waters Alliance 2699 separation module, Waters 2998 photodiode array detector (Waters, Milford, Massachussets, USA). Analytical separations were performed with Waters XTerraMsC18 column (2.1 × 50 mm, 2.5 µm) at 25 °C. Detection was performed at 440 nm and on-line uv-visible scans were performed. Flow rate was 0.2 mL min^{-1}. Injection volume was of 10 µL. The mobile phase was water/formic acid (0.1%) and acetonitrile/formic acid (0.1%). A linear gradient (curve 6) was applied from 75/25 to 25/75 in 10 min before applying a hyperbolic gradient (curve 2) (15 min) to the initial conditions.

High-pressure liquid chromatography-MS instrumentation

System 3 used for Table 3: the HPLC-MS analyses were performed with a HPLC system consisting of a Spectrasystem pump module P1000XR, autosampler AS3000 and uv-visible detector UV6000P, coupled to a TSQ mass spectrometer (Finnigan Mat). Analytical separations were performed with Waters XTerraMsC18 column (2.1 × 50 mm, 2.5 µm) at 25 °C. Detection was performed at 440 nm. Flow rate was 0.2 mL min^{-1}. Injection volume was of 100 µL. Mobile phase consisted of water (98.9%)/formic acid (0.1%)/acetonitrile (1%) and acetonitrile. A linear gradient was applied first from 75/25 to 25/75 in 10 min then back to the initial conditions in 2 min before equilibrating the column at the initial conditions. Mass spectra were acquired by using electrospray ionization (ESI) method in positive ion mode under the following conditions:

Full mass spectra. Sheath gas pressure, 27 lb in^{-2}; capillary temperature 280 °C; spray voltage, 3.7 kV; and tube lens offset, 234 V. Parameters. Scan Mode Q1 MS; First mass 150 *m/z* and last mass 1200 *m/z*; scan time 1 s; Q1 peak width 0.7.

Tandem mass spectra. Sheath gas pressure, 27 lb in^{-2}; capillary temperature 280 °C; spray voltage, 3.7 kV; and tube lens offset, 234 V. Parameters. Collision energy of 30 V; Q2 collision gas pressure (mTorr) 1.00; scan time 1 s; Q1 and Q3 peak widths 0.9.

Enzymatic oxidation for HPLC-MS studies

Briefly, the oxidations were run in 1 mL buffered water (0.2 M ammonium acetate) containing 1 mM of substrates. Laccase from *Trametes versicolor* (Aldrich, 38429) was purchased as a brownish powder with an activity of 0.83 Umg^{-1}. Unless otherwise mentioned, laccase activity was of 100 UL^{-1}. Samples were periodically taken, diluted in acetonitrile (1/2, v/v) and filtered on a syringe filter (0.22 μm) before injection in HPLC. Typically reactions were ended after 24 h before being analyzed by HPLC-MS and HPLC-PDA.

RHF and DFT Computational methods

The internal coordinates of all the molecules have been fully optimized at the RHF and B3LYP level using 6-31+G basis set with added polarization functions (B3LYP/6-31+G(d).[41,42] All the calculations have been performed with the Gaussian 03 program.[43]

Rigid docking

The X-ray crystal structure of laccase from PDB ID 1kya (*Trametes versicolor*) at a resolution of 2.4 Å was used for the active site model. Molegro Virtual Docker program was used to prepare the binding cavity. A docking template was set up to determine the constraints (15 Å around the ligand of reference, the key hydrogen bonds, the steric factors and the preferential position of the aromatic ring). The docking was set up using the default parameter (Moldock SE algorithm, Moldock score, similarity score, RMSD of 1 Å). Ten runs were programmed for each ligand from which the best 5 results were kept. The total MolDock Score energy (arbitrary units) is the sum of internal ligand energies, protein interaction energies and soft penalties.[39]

Acknowledgements

This research was supported in part by the European Commission, Sixth Framework Program (NMP2-CT2004-505899, SOPHIED), and in part by the UCL (Belgium) with the Concerted Research Program ARC 08/13-009 and the Inter-University Attraction Pôle (IAP) program P6/19 PROFUSA. J.M.-B. and G.D. are senior research associates of FRS-FNRS (Belgium). The authors wish to thank R. Rozenberg (Laboratoire de Spectrométrie de Masse, UCL) for technical assistance in the acquisition of the MS and HPLC-MS spectra. G. D. thanks the FRS-FNRS for access to HPC equipments installed in Liège and LLN.

Notes and references

‡As the HPLC-MS chromatographic system was equipped with a smaller XTerraMsC18 column (2.1 × 50 mm, 2.5 μm), the same column was used here with the HPLC-PDA systems. The reference dyes **5d**, **5f**, **6f**, and **5j** were eluted to check the consistency of the retention times due to the decrease of both the flow rate and the column dimensions (see Table 3, footnotes).

1 (*a*) S. A. Waksman and H. B. Woodruff, *Proc. Soc. Exp. Biol. Med.*, 1940, **45**, 609–614; (*b*) H. Brockmann, *Fortschr. Chem. Org. Naturst.*, 1960, **18**, 1–54; (*c*) H. Brockmann, *Angew. Chem.*, 1960, **72**, 939–947; (*d*) H. Nakazawa, F. E. Chou, P. A. Andrews and N. R. Bachur, *J. Org. Chem.*, 1981, **46**, 1493–1496.
2 (*a*) G. W. Cavill, P. S. Clezy, J. R. Tetaz and R. L. Werner, *Tetrahedron*, 1959, **5**, 275–280; (*b*) W. Schaefer, *Prog. Org. Chem*, 1964, **6**, 135; (*c*) M. Ionescu and H. Mantsch, *Adv. Heterocycl. Chem.*, 1967, **8**, 83; (*d*) O. Crescenzi, G. Correale, A. Bolognese, V. Piscopo, M. Parrilli and V. Barone, *Org. Biomol. Chem.*, 2004, **2**, 1577–1581 and references therein.
3 (*a*) E. Delfourne, F. Darro, N. Bontemps-Subielos, C. Decaestacker, J. Bastide, A. Frydman and R. Kiss, *J. Med. Chem.*, 2001, **44**, 3275; (*b*) A. Bolognese, G. Correale, M. Manfra, A. Lavecchia, O. Mazzoni, E. Novellino, V. Barone, P. La Colla and R. Loddo, *J. Med. Chem.*, 2002, **45**, 5217.
4 R. P. Maskey, F. C. Li, S. Quin and H. H. Fiebig, *J. Antibiot.*, 2003, **56**, 622–629.
5 (*a*) H. Suzuki, Y. Furusho, T. Higashi, Y. Ohnishi and S. Horinouchi, *J. Biol. Chem.*, 2006, **281**, 824–833; (*b*) E. Graf, K. Schneider, G. Nicholson, M. Strobele, A. L. Jones, M. Goodfellow, W. Beil, R. D. Süssmuth and H. P. Fiedler, *J. Antibiot.*, 2007, **60**, 277–284.
6 G. Carr, W. Tay, H. Bottriell, S. K. Andersen, A. Grant Mauk and R. J. Andersen, *Org. Lett.*, 2009, **11**, 2996–2999.
7 (*a*) P. B. Gomes, M. Nett, H. M. Dashe, I. Sattler, K. Martin and C. Hertweck, *Eur. J. Org. Chem.*, 2010, 231–235; (*b*) P. B. Gomes, M. Nett, H. M. Dashe and C. Hertweck, *J. Nat. Prod.*, 2010, **73**, 1461–1464.
8 C. E. Barry, P. G. Nayar and T. P. Begley, *Biochemistry*, 1989, **28**, 6323–6333.
9 (*a*) C. Eggert, U. Temp, J. F. D. Dean and K. E. L. Eriksson, *FEBS Lett.*, 1995, **376**, 202–206; (*b*) J. Osiadacz, A. J. H. Al-Adhami, D. Bajraszewska, P. Fischer and W. Peczynska-Czoch, *J. Biotechnol.*, 1999, **72**, 141–149; (*c*) K. Li, P. S. Horanyi, R. Collins, R. S. Phillips and K. E. L. Eriksson, *Enzyme Microb. Technol.*, 2001, **28**, 301–307.
10 M. Le Roes-Hill, C. Goodwin and S. Burton, *Trends Biotechnol.*, 2009, **27**, 248–258.
11 (*a*) S. Burton, *Curr. Org. Chem.*, 2003, **7**, 1317–1331; (*b*) S. Witayakran and A. J. Ragauskas, *Adv. Synth. Catal.*, 2009, **351**, 1187–1209; (*c*) F. Hollman, I. W. C. E. Arends, K. Buehler, A. Schallmey and B. Bühler, *Green Chem.*, 2011, **13**, 226–265; (*d*) T. Kudanga, G. S. Nyanhogo, G. M. Guebitz and S. Burton, *Enzyme Microb. Technol.*, 2011, **48**, 195–208.
12 (*a*) F. Bruyneel, E. Enaud, L. Billottet, S. Vanhulle and J. Marchand-Brynaert, *Eur. J. Org. Chem.*, 2008, **1**, 71–79; (*b*) F. Bruyneel, O. Payen, A. Rescigno, B. Tinant and J. Marchand-Brynaert, *Chem.–Eur. J.*, 2009, **15**, 8283–8295; (*c*) S. Forte, J. Polak, D. Valensin, M. Taddei, R. Basosi, S. Vanhulle, A. Jarosz-Wilkolazka and R. Pogni, *J. Mol. Catal. B: Enzym.*, 2010, **63**, 116–120; (*d*) F. Bruyneel, L. D'Auria, O. Payen, P. J. Courtoy and J. Marchand-Brynaert, *ChemBioChem*, 2010, **11**, 1451–1457.
13 (*a*) S. Hajdok, H. Leutbecher, G. Greiner, J. Conrad and U. Beifuss, *Tetrahedron Lett.*, 2007, **48**, 5073–5076; (*b*) S. Witayakran and A. J. Ragauskas, *Green Chem.*, 2007, **9**, 475–480; (*c*) S. Hajdok, J. Conrad, H. Leutbecher, S. Strobel, T. Schleid and U. Beifuss, *J. Org. Chem.*, 2009, **74**, 7230–7237; (*d*) V. Hahn, T. Davids, M. Lalk, F. Schauer and A. Mikolasch, *Green Chem.*, 2010, **12**, 879–887.
14 (*a*) A. Rescigno and E. Sanjust, Atta-ur-Rahman (Ed.) *Studies in Natural Products Chemistry, Vol.26*, Elsevier Science B. V., Amsterdam, 2002, 965–1028; (*b*) E. Sanjust, G. Cecchini, F. Sollai, N. Curreli and A. Rescigno, *Arch. Biochem. Biophys.*, 2003, **412**, 272–278.
15 (*a*) E. I. Solomon, U. M. Sudaram and T. E. Machonkin, *Chem. Rev.*, 1996, **96**, 2563–2605; (*b*) E. I. Solomon, R. K. Szilagi, S. D. George and L. Basumallick, *Chem. Rev.*, 2004, **104**, 419–458; (*c*) L. Quintanar, C. Stoj, A. B. Taylor, P. J. Hart, D. J. Kosman and E. I. Solomon, *Acc. Chem. Res.*, 2007, **40**, 445–452 and reference herein (*d*) C. F. Thurston, *Microbiology*, 1994, **140**, 19–26.
16 J. C. Freeman, P. G. Nayar, T. P. Begley and J. J. Villafranca, *Biochemistry*, 1993, **32**, 4826–4830.
17 (*a*) D. J. Kosman, *JBIC, J. Biol. Inorg. Chem.*, 2010, **15**, 15–28; (*b*) P. Giardina, V. Faraco, C. Pezzella, A. Piscitelli, S. Vanhulle and G. Sannia, *Cell. Mol. Life Sci.*, 2010, **67**, 369–385.
18 (*a*) W. Smith, A. Camara-Artigas, M. Wang, J. P. Allen and W. A. Francisco, *Biochemistry*, 2006, **45**, 4378–4387.
19 (*a*) J. Reynisson and S. Steenken, *Org. Biomol. Chem.*, 2004, **2**, 578–584; (*b*) M. A. Tadesse, A. D'Annibale, C. Galli, P. Gentili and F. Sergi, *Org. Biomol. Chem.*, 2008, **6**, 868–878; (*c*) S. Bin Mohamad, A. Ling Ong and A. Mat Ripen, *Bioinformation*, 2008, **2**, 369–372.

20 (*a*) K. Pionteck, M. Antorini and T. Choinowski, *J. Biol. Chem.*, 2002, **277**, 37663–37669; (*b*) T. Bertrand, C. Jolivalt, P. Briozzo, E. Caminade, N. Joly, C. Madzak and C. Mougin, *Biochemistry*, 2002, **41**, 7325–7333; (*c*) F. J. Enguita, D. Marcal, L. O. Martins, R. Grenha, A. O. Henriques, P. F. Lindley and M. A. Carrondo, *J. Biol. Chem.*, 2004, **279**, 23472–23476; (*d*) N. Hakulinen, L.-L. Kiiskinen, K. Kruus, M. Sloheimo, A. Paananen, A. Koivula and J. Rouvinen, *Nat. Struct. Biol Letters*, 2002, **9**, 601–605; (*e*) I. Matera, A. Gullotto, S. Tilli, M. Ferraroni, A. Scozzafava and F. Briganti, *Inorg. Chim. Acta*, 2008.

21 H. Iwahashi, *J. Chromatogr., Biomed. Appl.*, 1999, **736**, 237–245.

22 M. Lahtinen, K. Kruus, H. Boer, M. Kemell, M. Andberg, L. Viikari and J. Sipilä, *J. Mol. Catal. B: Enzym.*, 2009, **57**, 204–210.

23 G. I. Giles, C. A. Collins, T. W. Stone and C. Jacob, *Biochem. Biophys. Res. Commun.*, 2003, **300**, 719–724.

24 (*a*) R. Sripriya, M. Chandrasekaran and M. Noel, *Colloid Polym. Sci.*, 2006, **285**, 39–48; (*b*) C. Hansch, A. Leo and R. W. Taft, *Chem. Rev.*, 1991, **91**, 165–195; (*c*) D. Job and H. B. Dunford, *Eur. J. Biochem.*, 1976, **66**, 607–614.

25 (*a*) M. Nakatani, M. Hibi, M. Minoda, J. Ogawa, K. Yokozeki and S. Shimizu, *New Biotechnol.*, 2010, **27**, 317–323; (*b*) S. Kurniawati and J. A. Nicell, *Bioresour. Technol.*, 2008, **99**, 7825–7834.

26 M. Trovaslet, E. Enaud, A. Baze, C. Jolivalt, F. Van Hove and S. Vanhulle, *Chemical Engineering Transaction*, 2008, **14**, 315.

27 (*a*) D. M. Soden and A. D. W. Dobson, *Microbiology*, 2001, **147**, 1755–1763; (*b*) P. Zucca, A. Rescigno, A. Olianas, S. Maccioni, F. A. Sollai and E. Sanjust, *J. Mol. Catal. B: Enzym.*, 2010, **68**, 216–222.

28 M. T. Cambria, D. D. Marino, M. Falconi, S. Garavaglia and A. Cambria, *J. Biomol. Struct. Dyn.*, 2010, **27** (4), 501–509.

29 Rescigno, F. Bruyneel, A. Padiglia, F. Sollai, A. Salis, J. Marchand-Brynaert and E. Sanjust, *Biochem. Biophys. Acta*, 2011, 1810, **8**, 799–807.

30 (*a*) J. J. Reddick, J. Cheng and W. Roush, *Org. Lett.*, 2003, **5**, 1967–1970; (*b*) D. Enders and K. Hoffman, *Eur. J. Org. Chem.*, 2009, 1665–1668.

31 L. R. Domingo, J. A. Saez, C. Palmucci, J. Sepulveda-Arques and E. Gonzalez-Rosende, *Tetrahedron*, 2006, **62**, 10408–10416.

32 (*a*) M. K. Manthey, S. G. Pyne and R. J. W. Truscott, *Biochim. Biophys. Acta, Gen. Subj.*, 1990, **1034**, 207–212; (*b*) L. A. Hick, M. K. Manthey and R. J. W. Truscott, *J. Heterocycl. Chem.*, 1991, **28**, 1157; (*c*) S. Christen, P. T. Southwell-Keely and R. Stocker, *Biochemistry*, 1992, **31**, 8090–8097; (*d*) K. Maruyama, T. Moriguchi, T. Mashino and A. Nishinaga, *Chem. Lett.*, 1996, 819–820.

33 (*a*) T. M. Simandi, L. I. Simandi, M. Gyor, A. Rockenbauer and A. Gomory, *Dalton Trans.*, 2004, 1056–1060; (*b*) T. M. Simandi, Z. May, I. Cs. Szigyarto and L. I. Simandi, *Dalton Trans.*, 2005, 365–368.

34 O. Toussaint and K. Lerch, *Biochemistry*, 1987, **26**, 5867–8571.

35 M. T. Wu and R. E. Lyle, *J. Heterocycl. Chem.*, 1971, **8**, 989–991.

36 (*a*) B. Brogni, D. Biglino, A. Sinicropi, E. J. Reijerse, P. Giardina, G. Sannia, W. Lubitz, R. Basosi and R. Pogni, *Phys. Chem. Chem. Phys.*, 2008, **10**, 7284–7292; (*b*) D. Nematollahi, D. Habibi, M. Rahmati and M. Rafiee, *J. Org. Chem.*, 2004, **69**, 2637–2640.

37 F. D'Acunzo, C. Galli, P. Gentili and F. Sergi, *New J. Chem.*, 2006, **30**, 583–591.

38 (*a*) M. H. Hao, O. Haq and I. Muegge, *J. Chem. Inf. Model.*, 2007, **47**, 2242–2252; (*b*) K. A. Brameld, B. Kuhn, D. C. Reuter and M. Stahl, *J. Chem. Inf. Model.*, 2008, **48**, 1–24.

39 Friesner *et al.*, *J. Med. Chem.*, 2004, **47**, 1739–1749; see http://www.molegro.com/mvd-technology.php for selected recent publications using Molegro virtual docker program.

40 PyMOL(TM) Incentive Product - Copyright (C) 2006 DeLano Scientific LLC.

41 M. M. Francl, W. J. Pietro, W. J. Hehre, J. S. Binkley, D. J. DeFrees, J. A. Pople and M. S. Gordon, *J. Chem. Phys.*, 1982, **77**, 3654–3666.

42 T. Clark, J. Chandrasekhar, G. W. Spitznagel and P. v. R. Schleyer, *J. Comput. Chem.*, 1983, **4**, 294–301.

43 *Gaussian 03, Revision D.02*, M. J. Frisch, G. W. Trucks, H. B. Schlegel, G. E. Scuseria, M. A. Robb, J. R. Cheeseman, J. A. Montgomery, Jr., T. Vreven, K. N. Kudin, J. C. Burant, J. M. Millam, S. S. Iyengar, J. Tomasi, V. Barone, B. Mennucci, M. Cossi, G. Scalmani, N. Rega, G. A. Petersson, H. Nakatsuji, M. Hada, M. Ehara, K. Toyota, R. Fukuda, J. Hasegawa, M. Ishida, T. Nakajima, Y. Honda, O. Kitao, H. Nakai, M. Klene, X. Li, J. E. Knox, H. P. Hratchian, J. B. Cross, C. Adamo, J. Jaramillo, R. Gomperts, R. E. Stratmann, O. Yazyev, A. J. Austin, R. Cammi, C. Pomelli, J. W. Ochterski, P. Y. Ayala, K. Morokuma, G. A. Voth, P. Salvador, J. J. Dannenberg, V. G. Zakrzewski, S. Dapprich, A. D. Daniels, M. C. Strain, O. Farkas, D. K. Malick, A. D. Rabuck, K. Raghavachari, J. B. Foresman, J. V. Ortiz, Q. Cui, A. G. Baboul, S. Clifford, J. Cioslowski, B. B. Stefanov, G. Liu, A. Liashenko, P. Piskorz, I. Komaromi, R. L. Martin, D. J. Fox, T. Keith, M. A. Al-Laham, C. Y. Peng, A. Nanayakkara, M. Challacombe, P. M. W. Gill, B. Johnson, W. Chen, M. W. Wong, C. Gonzalez and J. A. Pople, Gaussian Inc, Wallingford CT, 2004

